

Applied Optics

Optical Technology and Biomedical Optics



MASERATI: a rocketborne tunable diode laser absorption spectrometer

Franz-Josef Lübken, Florian Dingler, Henrich von Lucke, Joachim Anders, Wolfgang J. Riedel, and Helmut Wolf

The MASERATI (middle-atmosphere spectrometric experiment on rockets for analysis of trace-gas influences) instrument is, to our knowledge, the first rocket-borne tunable diode laser absorption spectrometer that was developed for *in situ* measurements of trace gases in the middle atmosphere. Infrared absorption spectroscopy with lead salt diode lasers is applied to measure water vapor and carbon dioxide in the altitude range from 50 to 90 km and 120 km, respectively. The laser beams are directed into an open multiple-pass absorption setup (total path length 31.7 m) that is mounted on top of a sounding rocket and that is directly exposed to ambient air. The two species are sampled alternately with a sampling time of 7.37 ms, each corresponding to an altitude resolution of approximately 15 m. Frequency-modulation and lock-in techniques are used to achieve high sensitivity. Tests in the laboratory have shown that the instrument is capable of detecting a very small relative absorbance of 10^{-4} – 10^{-5} when integrating spectra for 1 s. The instrument is designed and qualified to resist the mechanical stress occurring during the start of a sounding rocket and to be operational during the cruising phase of the flight when accelerations are very small. Two almost identical versions of the MASERATI instrument were built and were launched on sounding rockets from the Andøya Rocket Range (69 °N) in northern Norway on 12 October 1997 and on 31 January 1998. The good technical performance of the instruments during these flights has demonstrated that MASERATI is indeed a new suitable tool to perform rocket-borne *in situ* measurements in the upper atmosphere. © 1999 Optical Society of America

OCIS codes: 010.1280, 120.6200, 140.2020, 300.1030, 300.6260.

1. Introduction

The concentration of water vapor in the mesosphere is critically determined by photochemical processes and by transport through convection, advection, and turbulence. Therefore a measured water-vapor profile allows for a sensitive test of theoretical models that combine both atmospheric dynamics and chemistry. During summer, the existence of various layers such as noctilucent clouds and polar mesospheric summer echoes is critically dependent on the water vapor concentration.^{1,2} Despite the prominent scientific importance, *in situ* measurements of water vapor are rather sparse and contradictory.³ We

therefore proposed in the early 1990's to apply laser absorption spectroscopy with tunable diode lasers to measure the concentration of water vapor in the mesosphere.⁴ The instrument is labeled MASERATI (middle-atmosphere spectrometric experiment on rockets for analysis of trace-gas influences) and is designed to measure water vapor and CO₂ simultaneously in the mesosphere and lower thermosphere (MLT).

There are several scientific reasons for measuring CO₂: Since it is well mixed up to turbopause heights⁵ it serves as a reference to derive water-vapor mixing ratios from number densities. Furthermore, radiation in the 15- μ m band of CO₂ is the most important cooling mechanism in the middle atmosphere. Above 80 km the corresponding vibration levels are presumably not in local thermodynamic equilibrium (LTE) with the atmosphere, i.e., the population of the excited levels deviates from the Boltzmann distribution inferred from the atmospheric kinetic gas temperature.⁶ MASERATI has the potential to measure non-LTE effects by comparing vibrational temperatures deduced from appropriate CO₂ lines with gas kinetic temperatures simulta-

F.-J. Lübken (luebken@physik.uni-bonn.de), F. Dingler, and H. von Lucke are with the Physikalisches Institut, Universität Bonn, Nussallee 12, 53115 Bonn, Germany. J. Anders, W. J. Riedel, and H. Wolf are with the Fraunhofer Institut für Physikalische Messtechnik, Heidenhofstrasse 8, 79110 Freiburg, Germany.

Received 16 March 1999; revised manuscript received 17 June 1999.

0003-6935/99/255338-12\$15.00/0

© 1999 Optical Society of America

neously measured by different methods (e.g., by falling spheres⁷). This intercomparison allows us to quantify the influence of non-LTE effects on the radiative cooling efficiency of CO₂.

Last but not least, the CO₂ data allow us to extract information about turbulence in the upper atmosphere: From the decrease of the CO₂ mixing ratio with altitude around turbopause heights we intend to derive the mean turbulent mixing coefficient, called the eddy diffusion coefficient K .⁸ In addition, small-scale fluctuations of the CO₂ number density are analyzed in terms of turbulent velocities and may lead to geophysical parameters, such as the turbulent energy dissipation rate ϵ .⁹ The intercomparison of ϵ and K allows us to distinguish between the actual strength of turbulence measured during the flight and the long-term mixing effect of turbulence.

The quantitative analysis of trace gases with tunable diode laser absorption spectroscopy has become a common technique in atmospheric physics and chemistry over the past 10–20 years.¹⁰ It has a wide range of applications, from detecting air pollution in the lower troposphere to analyzing photochemical processes in the stratosphere by airplane- and balloon-borne instruments.^{11,12} To perform *in situ* measurements in the MLT, the instrument must be mounted on a sounding rocket. This requires special precautions during the design and the construction phases of all instrumental components since large mechanical stress is experienced during the acceleration phase of the rocket. Still, the MASERATI instrument must be capable of detecting small relative absorptions since the total pressure in the MLT is small and the mixing ratio of water vapor is of the order of 0.5–5 parts in 10⁶ by volume (ppmv) only. A detailed analysis of the expected signal strength showed that relative absorptions as low as 10^{−4}–10^{−5} need to be detected, which is state of the art for laboratory experiments but is difficult to realize for a rocketborne instrument.

In this paper we report on the instrumental and technical aspects of MASERATI, which was designed built, and tested for an application on a sounding rocket called RONALD (rocketborne optical neutral gas analyzer with laser diodes). After describing the basic instrumental method in Section 2, we give an overview of the RONALD payload in Section 3. Details of the MASERATI mechanics, optics, and electronics are discussed in Section 4. Some innovative components, such as an open multiple-pass absorption setup, are described. In Section 5 we present results from laboratory tests and calibrations. Finally, we demonstrate the MASERATI flight performance in Section 6 and show first results from the rocket flights performed during winter 1997/1998 from northern Norway.

2. Experimental Method and Line Selection Criteria

Tunable diode laser absorption spectroscopy is based on Lambert–Beer's law, which describes the absorp-

tion of a laser beam with frequency ν that traverses through a gas with number density n :

$$I(\nu) = I_0(\nu)\exp[-\sigma(\nu)nl], \quad (1)$$

where I_0 and I are the incident and the transmitted intensities, respectively, l is the length of the light path through the absorbing gas, and $\sigma(\nu)$ is the frequency-dependent absorption cross section of the gas. The diode laser frequency is coarsely tuned by adjusting its temperature, whereas the absorption line is scanned by changing the injection current. Once an appropriate absorption line has been identified and the optimum laser parameters, i.e., its temperature and current, have been found, the laser temperature is stabilized within a few millidegrees Kelvin, and the laser mean frequency is line locked to an absorption line from a reference cell that contains comparatively large amounts of the gas being measured. In the MASERATI instrument two gases are detected by two independent lasers that are operated in a time-multiplex mode, i.e., they are alternately switched on and off by application of appropriate laser currents.

To achieve the desired sensitivity, the MASERATI instrument applies frequency-modulation spectroscopy, i.e., the emission frequency of each of the two lasers is modulated with 500 kHz and the second harmonic signal at 1 MHz ($2f$ signal) is detected with the lock-in technique. The $2f$ signal is closely related to the second derivative of the transmission spectrum. This method significantly reduces the noise level and increases the detection limit by at least 1 order of magnitude.¹³ The instrument is calibrated in the laboratory by measurement of the $2f$ signal as a function of gas concentration. We have used various calibration modes to measure and test the sensitivity and the stability of the MASERATI instrument under different conditions. Details are described in Section 5.

We need to take various aspects into account when selecting appropriate absorption lines. For H₂O the strongest line is wanted in order to obtain the largest possible signal and to retrieve number densities to maximum altitudes. For CO₂ a compromise has to be made to avoid saturation in the lower mesosphere and still get strong absorption in the lower thermosphere. An additional constraint on the CO₂ line is imposed by the fact that CO₂ densities are used to derive water-vapor mixing ratios from measured H₂O number densities. A CO₂ line is selected that has a temperature dependence similar to that of the H₂O line for the following reason: Temperature and pressure changes occur in the region downstream of the bow shock, which develops in front of the rocket when it cruises with supersonic speed. Choosing a H₂O and a CO₂ line with similar temperature dependences minimizes the effect of this disturbance on the water-vapor number density measurements.

As mentioned above we also want to investigate non-LTE effects in the population of the CO₂ levels. This requires that two lines be detected simulta-

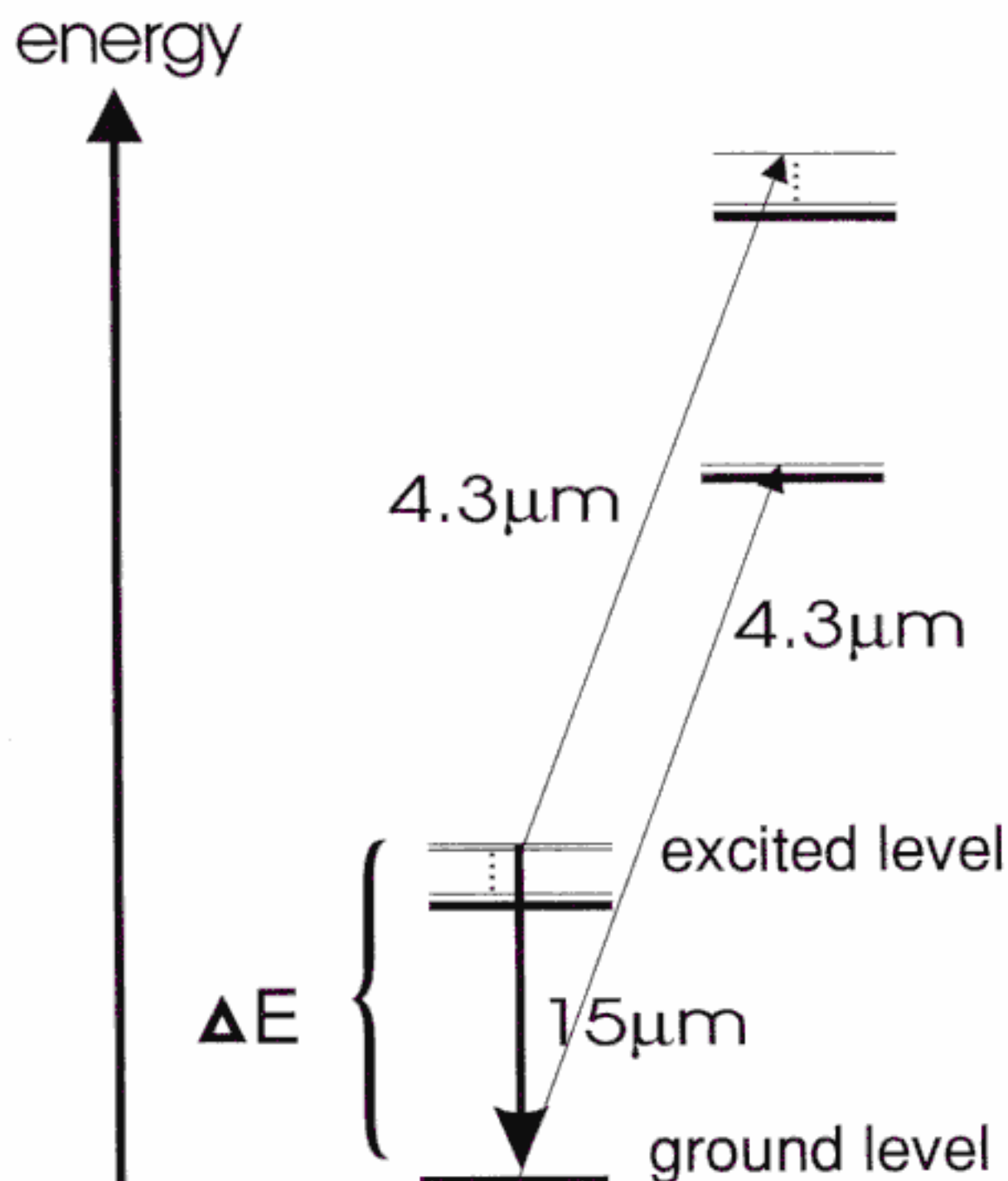


Fig. 1. Schematics of the CO_2 energy levels (not to scale) in the $4.3\text{-}\mu\text{m}$ band indicating the two transitions used in the MASERATI instrument. Two absorption lines from a ground level and an excited level were chosen to allow for the measurement of temperatures and the detection of non-LTE effects in the lower thermosphere.

neously that originate from the ground and an excited state and that are close enough in frequency to be detected in one laser scan. In Fig. 1 the energy levels and transitions used in the MASERATI instrument are shown. Two CO_2 lines in the $4.3\text{-}\mu\text{m}$ band have been selected: one originates from the vibration ground level and the second from the first excited vibrational level. The population of the latter (relative to the ground level) is deduced from the ratio of the two absorption signals and is used to determine the vibrational temperature of the excited level. The deviation of the vibrational temperature from the kinetic temperature at altitudes above $\sim 85\text{--}90$ km is a measure of non-LTE effects in the CO_2 molecules.

3. RONALD Payload

The MASERATI instrument is mounted on top of a sounding rocket called RONALD (Fig. 2), a German-Norwegian collaborative project for middle atmosphere *in situ* studies. The two main instruments on RONALD are the MASERATI and the transmitter and receiver of laser light (TROLL). The TROLL measures atmospheric densities by Rayleigh scattering of laser light transmitted and received on the payload.¹⁴ The payload is equipped with a telemetry section (3) where the data from inside the payload are collected and transmitted to a ground station (the numbers given here and in the following section refer to Fig. 2). A sea recovery unit (4) consists of a para-

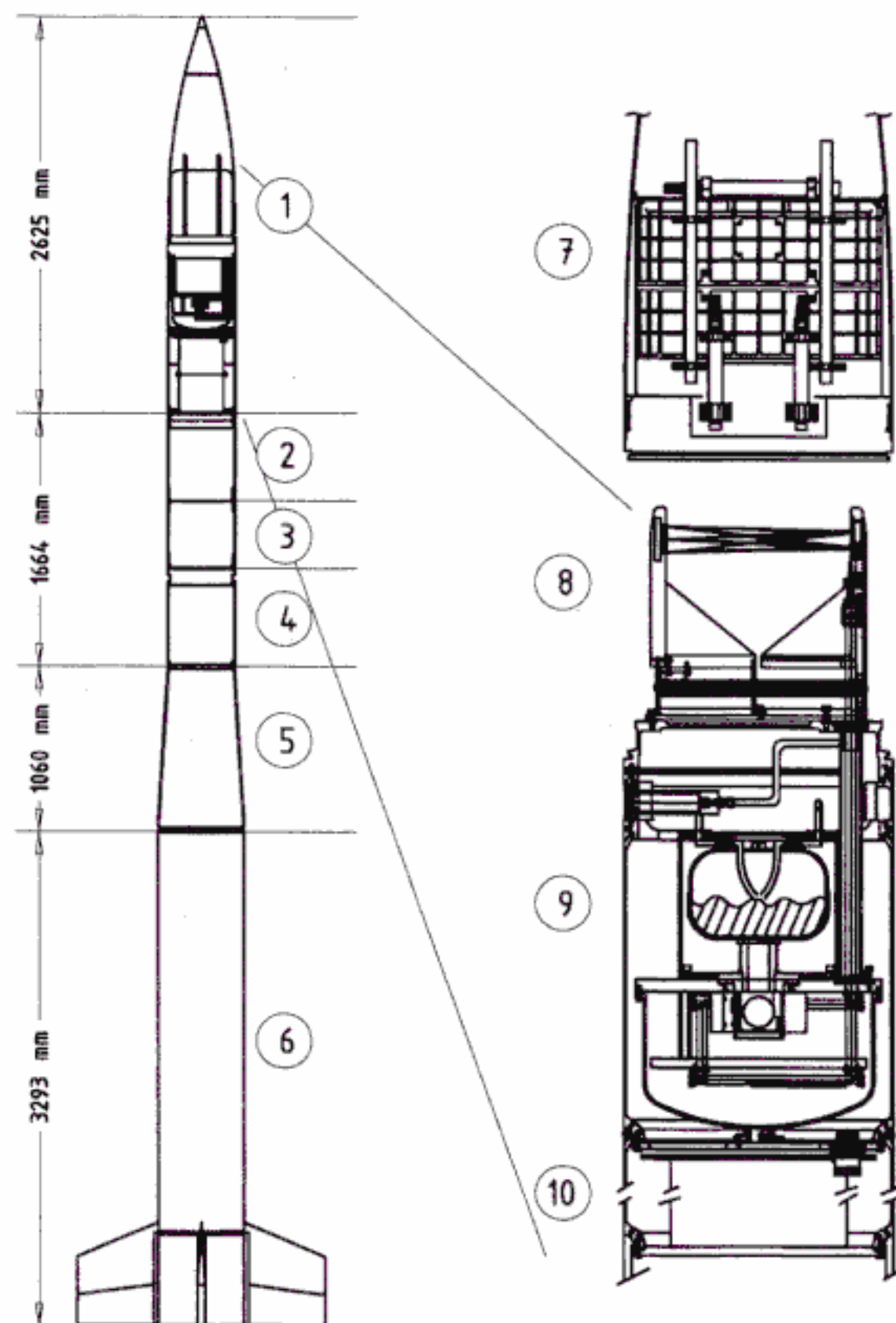


Fig. 2. Sketch of the RONALD payload and the MASERATI instrument: Apart from MASERATI (1) the other main instrument on board the payload is the transmitter and receiver of laser light (TROLL) (2). Furthermore, the payload consists of a telemetry section (3) and a recovery unit (4). A conical adapter (5) is used as an interface between the payload and the motor (6). More details on the MASERATI instrument section are given in the text (see Section 3).

chute to ensure deceleration in the final stage of the flight and a floatation bag to keep the payload at sea surface after impact. This payload section also contains a despin mechanism to reduce the spin of the payload during flight from 3 Hz to practically zero. The payload has a diameter of 438 mm and is attached to the motor (No. 6, $\varnothing 557$ mm) through a conical adapter (5). A Brazilian motor labeled S-30 transports the payload with a total mass of 390 kg (including motor adapter) to an apogee of ~ 120 km with maximum accelerations of 6–10 g during the first 29 s of the flight. Various events involving mechanics are happening during the flight (e.g., motor separation) that are described in Section 6.

4. MASERATI Instrument

A. MASERATI Mechanics

The MASERATI instrument consists of three main mechanical subsystems: the multiple-pass absorption setup (8), the laser and detector section (9), and the electronics section (10). The multiple-pass absorption setup (Fig. 3) ensures a long optical path to maximize absorption within minimum physical

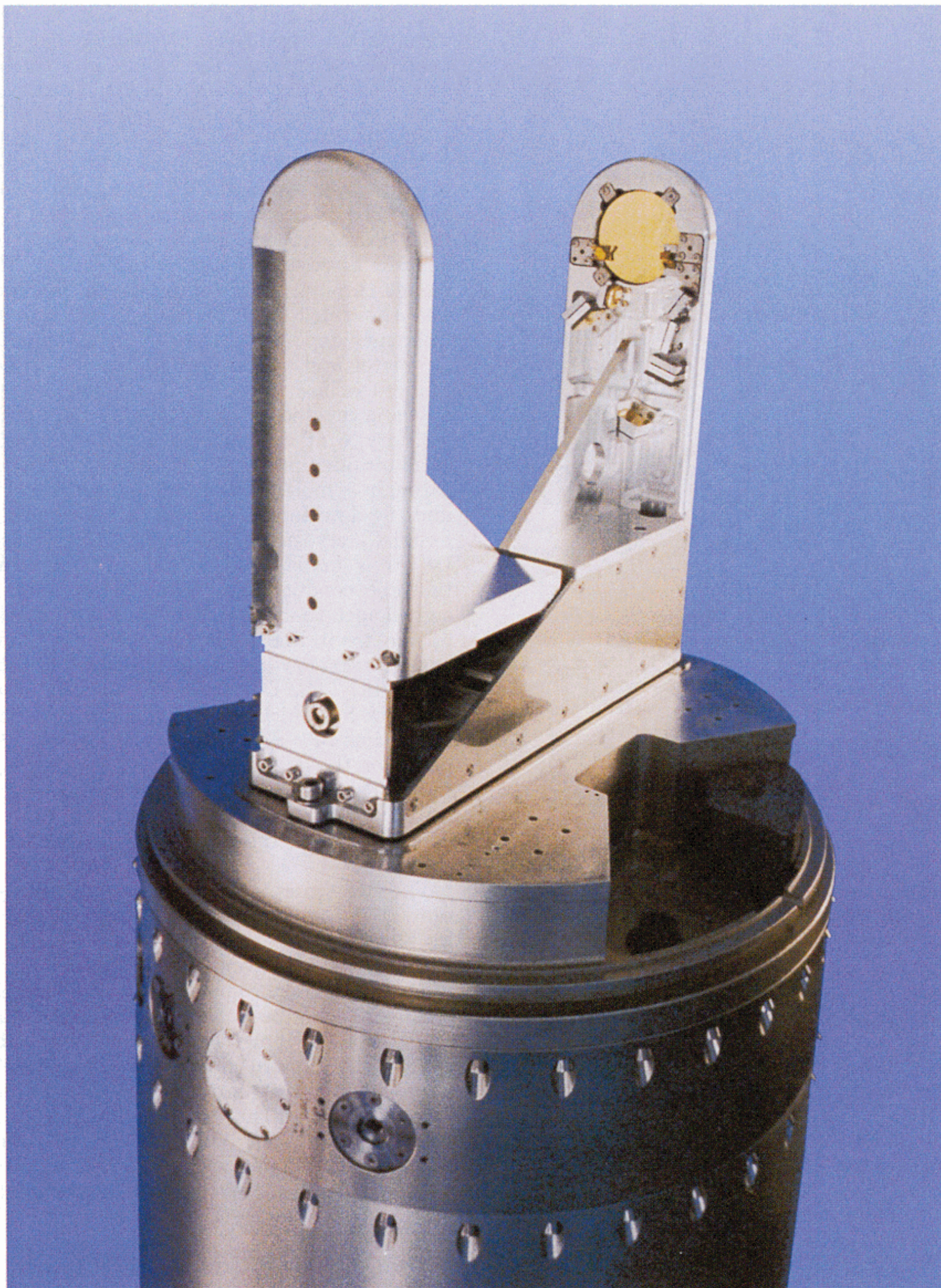


Fig. 3. Photograph of the open multiple-pass absorption setup on top of the MASERATI section.

space. Three spherical concave mirrors are mounted in the configuration proposed by White¹⁵ to achieve a total optical path length of 31.7 m (the optical design of this absorption cell is described in more detail in Subsection 4.B). Various support structures made of aluminum and carbon-fiber-enforced epoxy were installed to ensure the optical

and mechanical stability of the White cell. (Please note that we use the term White cell since it is generally used in the laser spectroscopy community, although the MASERATI multiple-pass absorption setup is *not* a closed gas cell.) Mechanical tests performed in the laboratory have shown that the laser beam traverses the White cell nicely, even at the

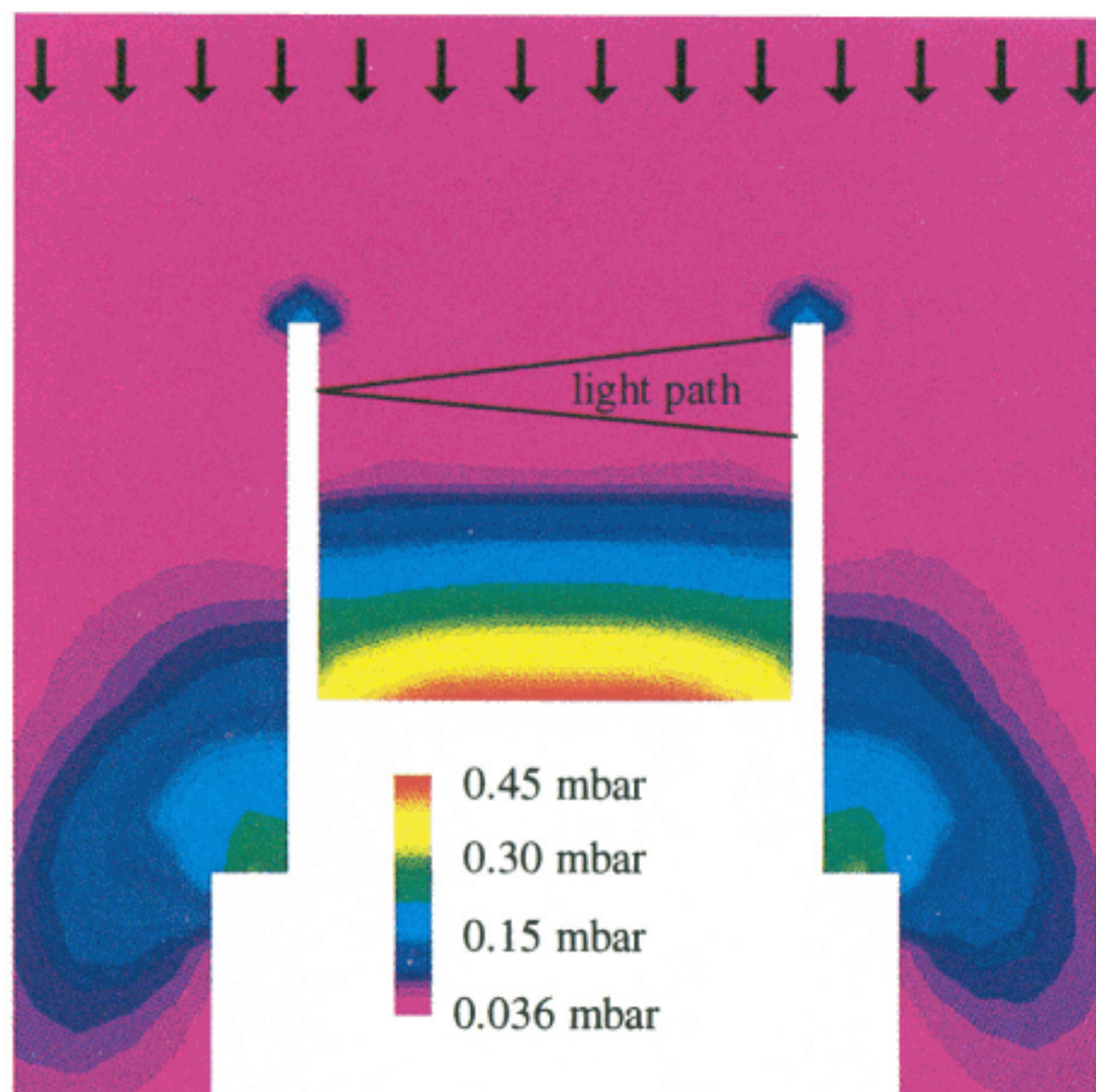


Fig. 4. Simulation of the gas flow at the top of the payload for conditions typically encountered during the upleg of the rocket flight. The path of the laser beam inside the multiple-pass absorption setup is indicated. The calculations have been performed for an altitude of 70 km, at which the rocket velocity is typically 990 m/s, the ambient pressure is 3.6×10^{-2} mbar, and the atmospheric temperature is typically 227 K. As can be seen from the color-coded pressure distribution, the main pressure increase caused by the supersonic motion of the rocket occurs downstream of the optical path. There is only very little disturbance at the light path inside the multiple-pass absorption setup. The calculations have been performed by means of a commercially available flow software (CFX 4.1, AEA Technology, U.K.).

strong vibrations and longitudinal and lateral accelerations expected during flight. During ground operation and in the first part of the flight, the White cell is protected by a so-called vacuum cover (7). This cover is mechanically attached to the rocket's nosecone, and both are ejected at an altitude of ~ 50 km. After ejection of the vacuum cover the multiple-pass absorption setup is directly flushed by ambient atmospheric air (no tubing, valves, pumps, etc.). This open design allows for very fast measurements (some milliseconds) since the air in the absorption path is replaced nearly instantaneously.

The mirrors of the White cell are placed at a considerable distance (336 mm) from the base deck to minimize disturbances that are due to ram effects. A shock front is generated during the main part of the flight since the rocket is cruising with supersonic speed. Using a commercially available flow software (CFX 4.1, AEA Technology, U.K.), we have performed aerodynamic calculations to make sure that on upleg the major part of the shock front is located downstream of the White cell so that the number densities in the absorption path of the lasers are practically not modified by ram effects. An example of such a calculation for typical conditions encountered during flight is shown in Fig. 4. The figure demonstrates that the shock front is located between

the light path and the payload body, i.e., outside the laser path. From these calculations we have quantitatively determined the influence of the bow shock on the absorption signals and arrived at a maximum enhancement of the water-vapor mixing ratios of less than $\sim 15\%$.

The laser and detector section (9) contains the two tunable diode lasers, the detectors, and various optics (described in more detail in Subsection 4.B). The laser beams are split into three different parts: One beam is directed through the White cell, the second passes through a reference gas cell for line locking, and the third part is used to analyze the laser frequency and the tuning rate by means of an interferometer and a monochromator. To avoid absorption of the laser beam inside the payload, the entire optics is covered by an evacuable tank that is filled with dry N_2 at atmospheric pressure. Low humidity is maintained inside the tank by circulating the gas through a molecular-adsorption sieve. The lasers and the detectors are cooled by a specially designed liquid- N_2 cryostat. The entire inner vessel of this Dewar is made of high-purity Cu to achieve high thermal conductivity. The Dewar has been designed such that it operates in any orientation (even upside down) and such that sufficient cooling is ensured during low-gravity conditions encountered during flight. The Dewar contains a maximum of 2.3 l of liquid N_2 , which corresponds to a maximum operation time of ~ 6 h. This is sufficient for the test period on the launcher and for the rocket flight of ~ 7 min. The Dewar is easily accessible from outside the payload and can be refilled in case the launch is delayed for technical reasons or because of bad weather.

The electronics is placed in a separate payload section (10 in Fig. 2) and consists of the sensor electronics, the telemetry interface, and the power supplies. More details are given in Subsection 4.C.

The mechanical components of the MASERATI instrument have been carefully designed, built, and tested to achieve high stability. On the other hand, the weight and the dimensions of the MASERATI have been kept at minimum so that it fits into the rocket payload. The total length of the entire instrument (including the White cell) is 1497 mm and the total mass is 112 kg (see Table 1 for a summary of the mechanical specifications of the instrument).

B. Optical Design

The optical layout of the MASERATI main platform is shown in the upper part of Fig. 5. The lead salt diode lasers with a typical output power of 100 μ W each are mounted in small mechanical supports that are thermally connected to the cold head of the liquid- N_2 Dewar. The divergent beam of each laser is collected by mirror objective assembly MO, which is adjustable in three orthogonal axes. An enlarged image of the laser, located in the entrance focal point of the MO, is formed in intermediate focal point IF. (See Ref. 16 for more details on the mirror objective and the alignment procedure of the spectrometer.)

Table 1. Mechanical Specifications of MASERATI

Number of lasers	2
Total mass	112 kg
Mass of electronics section	37 kg
Mass of White cell	7 kg
Mass of laser section	68 kg
Total length	1497 mm
Length of White cell	350 mm
Length of laser section	621 mm
Length of electronics section	526 mm
Distance between White cell mirrors	305 mm
Diameter of flange with White cell	438 mm
Maximum content of liquid N ₂	~2.31
Maximum operation time	~6 h

The divergent beam leaving the IF is collimated by off-axis paraboloid OAP. The beams of the two lasers are combined (optical multiplexing) by beam splitter BS 1. Beam splitters BS 1 and BS 2 split the combined laser beams into three parts. One part is fed into the multiple-pass absorption setup by plane mirror PM 1, reenters the platform at plane mirror PM 3, and is focused onto a HgCdTe detector. The second part of the laser beam is guided by plane mirror PM 2 to the second optical platform (lower panel of Fig. 5), where it is spectrally analyzed by means of a monochromator and an interferometer. From there plane mirror PM 5 (and further optics not discussed here) reflects the beam back to platform 1, where it is focused onto a second detector. Finally, the third part of the laser beam passes short reference gas cell GC and is then focused onto a third detector. This cell is filled with a sufficient amount of water vapor and CO₂ and is used for active line locking of the laser wavelengths.

The laser beam enters the second platform through plane mirror PM 4 (lower panel of Fig. 5). Part of the beam is fed into a Mach-Zehnder interferometer that consists of two beam splitters (BS 3 and BS 4) and four plane mirrors (MZ 1–MZ 4). The difference in the optical path lengths is 50 cm, corresponding to a free spectral range of 0.02 cm⁻¹. The remaining part of the laser beam is fed into a grating monochromator where wavelength selection is performed by turning echelette grating EG with stepper motor SM. The dispersion of the grating and the dimensions of the entrance and the exit pinholes (P1 and P2) are matched to achieve a spectral resolution of 1 cm⁻¹.

The main part of the laser beam leaves platform 1 through PM 1 and is fed into the White cell on top of the MASERATI section. The optical path through this cell is shown in Fig. 6. The laser beam is focused onto the entrance point of the White cell marked with 0' in Fig. 6(b). The multiple-pass absorption setup itself is a specially designed anastigmatic White cell^{17,18} with folding mirror assemblies. A base length of 305 mm and 104 passes through the absorption setup result in a total optical path length of 31.7 m. When leaving the White cell at the point marked 26 in Fig. 6(b), the divergent laser beam is collimated by off-axis paraboloid OAP and guided

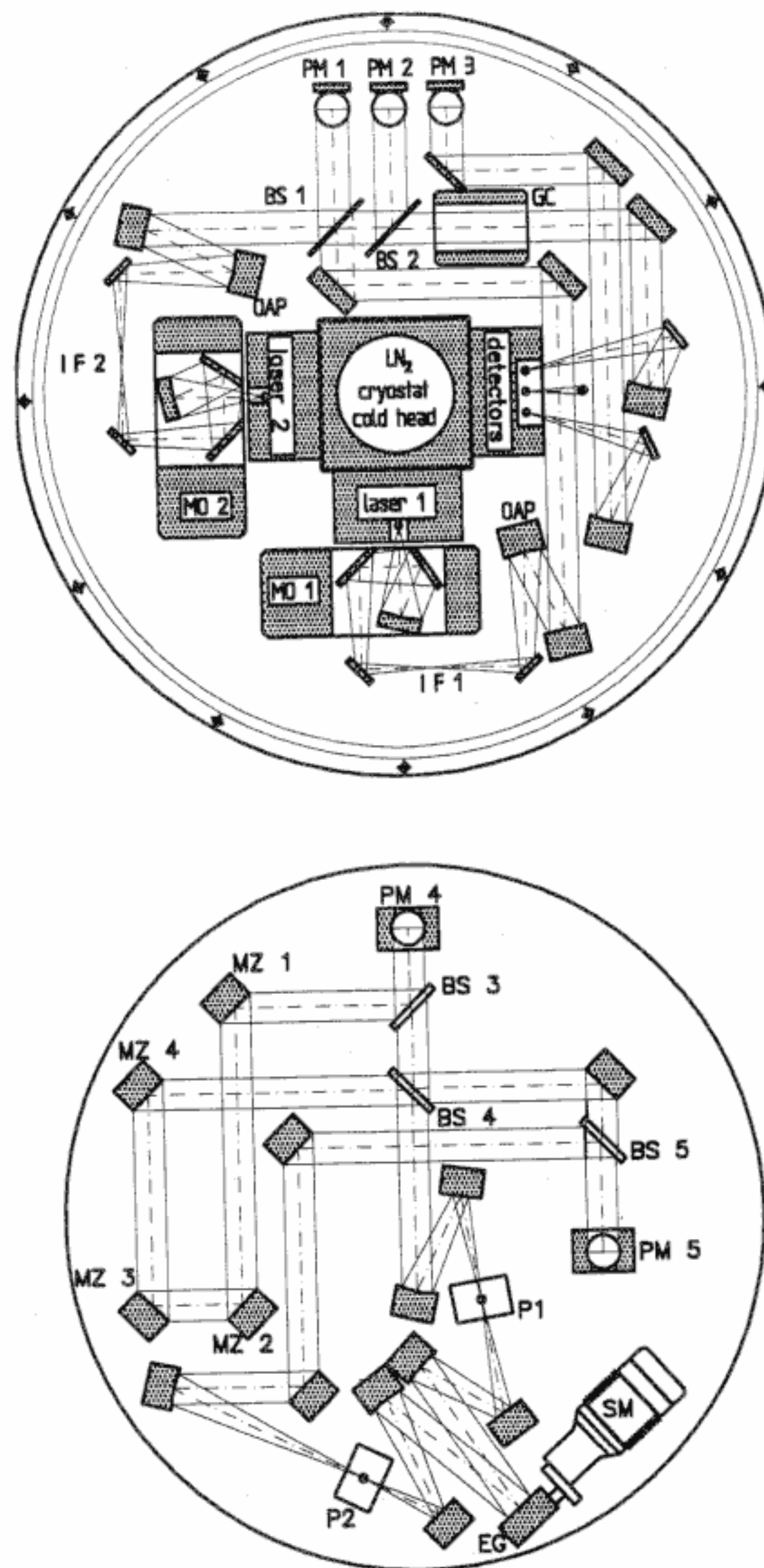


Fig. 5. Schematic sketch of the two optical platforms of the MASERATI instrument. Upper panel; cryostat with lasers and detectors and various optics to collimate and guide the beams to the multiple-pass absorption setup (not shown here) and to the second platform (lower panel). Details are described in Subsection 4.B. The second platform is used to determine the frequency and tuning rate of the lasers by means of a grating monochromator and a Mach-Zehnder interferometer (see text for definitions of abbreviations used).

back to the optical platform in the interior of the payload, where it is focused onto the detector.

C. Electronics

The main parts of the MASERATI electrical system are the sensor electronics, the telemetry interface, and the power supply (Fig. 7). The sensor electronics comprises the signal amplifiers as well as temperature and current controllers for both lasers. The temperature of each laser is actively controlled and stabilized so that it deviates by no more than a few millidegrees Kelvin from its nominal value. This is achieved by liquid-N₂ cooling and a control loop con-

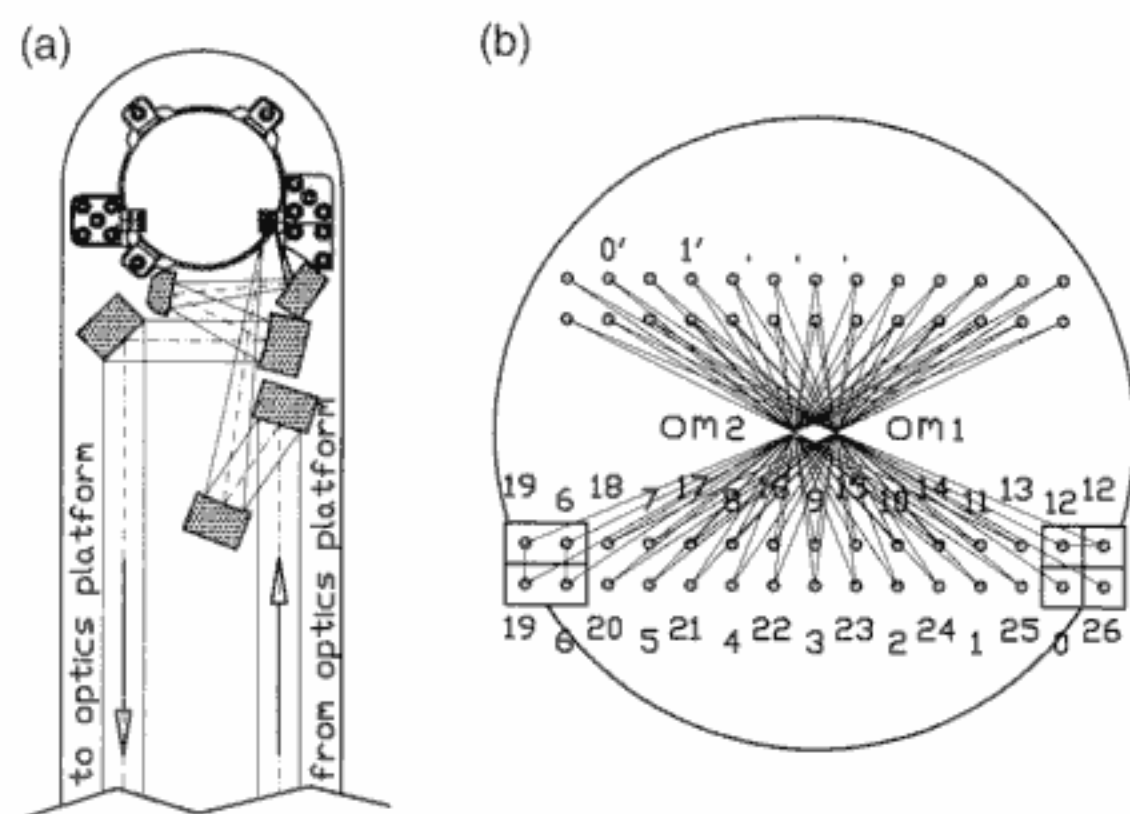


Fig. 6. Optical path through the MASERATI multiple-pass absorption setup: (a) field mirror and supporting optics, including mirrors to guide the laser beam into and out of the multiple-pass absorption setup; (b) projection of the central ray of the laser beam to the field mirror. The numbers denote the sequence of focal points on the field mirror. OM 1 and OM 2 denote the centers of curvature of the two objective mirrors.

sisting of a Pt resistance temperature measurement and a resistive heating.

The laser injection current consists of various components. A continuous bias current just below the lasing threshold keeps the laser diode in a standby mode. The laser is switched on by adding a pulse current that is varied in time in order to linearize the tuning rate of the laser. Furthermore, the laser current is adjusted to stabilize the

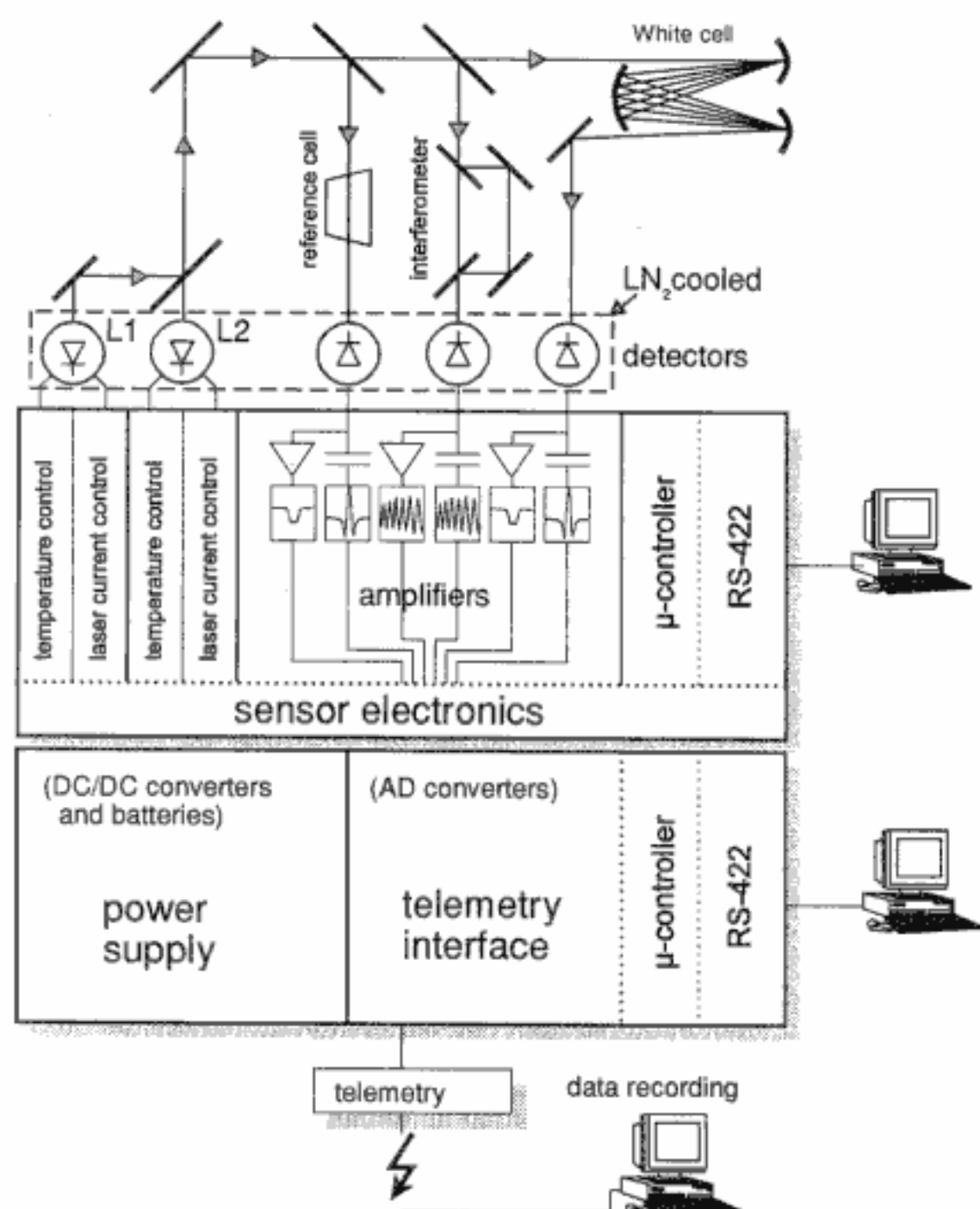


Fig. 7. Schematic diagram of the sensor and the MASERATI electronics that consist of three main subsystems: the sensor electronics, the telemetry interface including the analog-to-digital (AD) converters, and the power supply with the dc/dc converters and batteries.

Table 2. Electronics Specifications of the MASERATI Instrument

Input voltage	28 V
Input current	~2.2 A (3 A maximum)
Total power consumption	60 W
Scans per second per laser	68
Time for one laser scan	7.37 ms
Samplings per scan	64
A/D bit resolution	12
Total bit rate	434 kbit/s
TM bit rate	833 kbit/s
Maximum amplifier gain factor	$2^{14} = 16,384$

frequency scan with respect to the selected gas absorption line by using the absorption in the reference cell (line locking). Finally, the laser is modulated with 500 kHz to allow for derivative spectroscopy with lock-in detection.

The detector signals are analyzed in terms of ac and dc components. The ac part is processed by an amplifier chain consisting of a bandpass, a demodulation stage for phase sensitive detection, and a low-pass filter. Three amplifiers are used to allow for 15 selectable gains that differ by a factor of 2, i.e., the gain factors are 1, 2, 4, ..., 16 384. The dc signal amplifier chains have selectable gain factors of 1, 2, ..., 16 in order to adapt the signals to the input range of the ADCs.

The sensor electronics is controlled by an on-board microcontroller. During tests in the laboratory and on the rocket range this microcontroller communicates by means of an RS422 interface with the experimenter's personal computer. This allows us to change instrumental parameters such as laser temperatures, current pulses, and amplifier gain factors, even shortly before the rocket flight. During flight the amplifiers for the ac component of the atmospheric signal are switched automatically. Each scan is subdivided into 64 channels that are digitized with 12-bit analog-to-digital resolution (see Table 2 for details of the electronics specifications). The data are transferred to the telemetry section of the payload and transmitted to the ground by means of standard pulsed-code-modulation telemetry techniques.

The power supply in the MASERATI electronics mainly consists of dc-dc converters that generate various voltages required by the sensor electronics and the telemetry interface. During so-called internal operation, a battery package in the MASERATI section is used, whereas in the external operation mode the 28-V power source comes from outside the payload. The total power consumption of the MASERATI is typically 60 W.

5. Calibration and Laboratory Tests

A. Calibration Setup

A special vacuum system has been set up in our laboratory (Fig. 8) to test and calibrate the instruments in a wide range of water-vapor and CO₂ mixing ratios, total pressures, and gas temperatures. To pro-

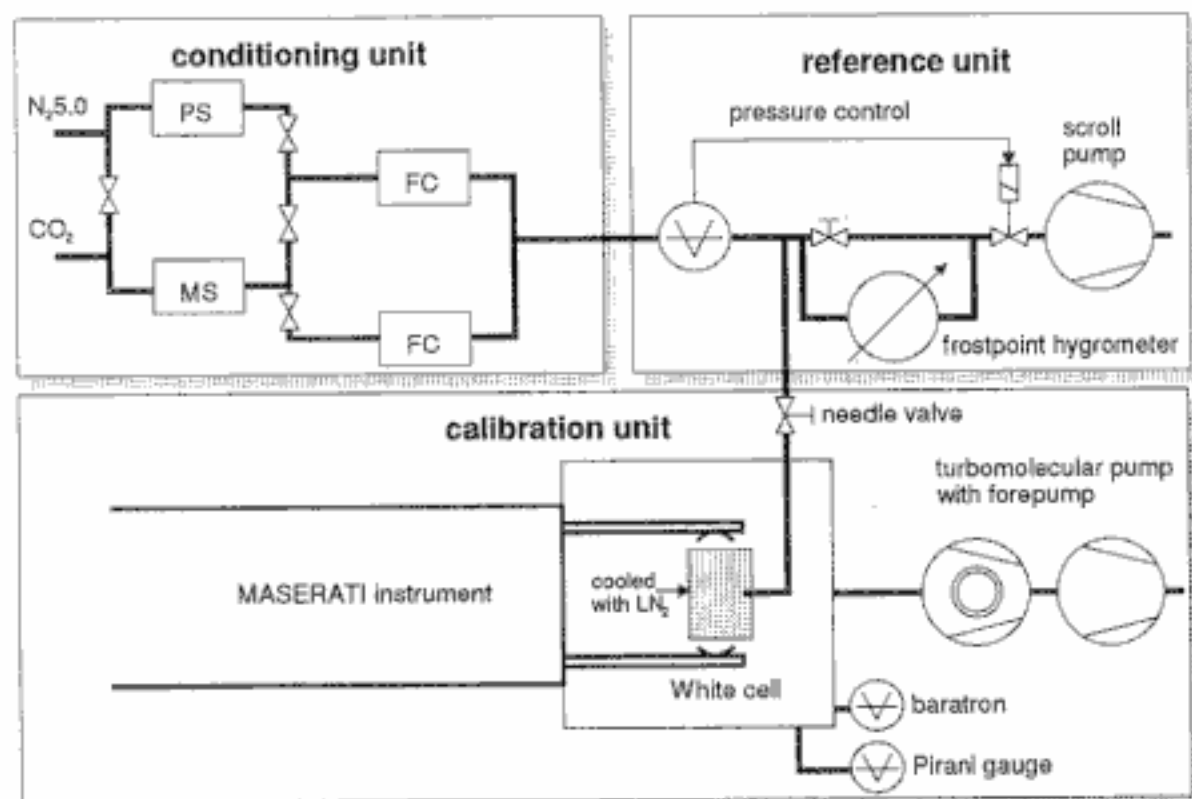


Fig. 8. Setup for the laboratory tests and calibrations of the MASERATI instrument. The calibration gas is prepared in the conditioning unit: gas samples with different water-vapor mixing ratios are provided by diluting the flow of permeation source PS with dry N_2 regulated by flow controller FC. The gas enters the main vacuum chamber through a needle valve that is used to control the total pressure inside the chamber. The temperature of the gas is varied by means of liquid- N_2 cooling. A frostpoint hygrometer in the reference unit is used to determine the water-vapor mixing ratio. To reduce the water-vapor background in the calibration system before calibration, N_2 gas is directed through molecular adsorption sieve MS instead of permeation source PS. Thereby a gas flow with water-vapor mixing ratios below 1 ppmv is achieved.

vide gas samples with different water-vapor mixing ratios, the flow of permeation source PS operating at a temperature of $\sim 50^\circ\text{C}$ (stability $<0.5^\circ\text{C}$) is diluted with dry N_2 , the amount of which is regulated by flow controller FC. The water-vapor abundance is measured by means of a frostpoint hygrometer. The CO_2 channel of MASERATI is calibrated with bottled gas with certified mixing ratios and further dilution with dry N_2 , if required.

Once the gas is prepared in the conditioning and reference unit (Fig. 8), it enters the main vacuum chamber through a needle valve that is used to change and control the total pressure inside the chamber. The main chamber is pumped by a turbomolecular pump with a forepump (both oil free). The pressure is roughly monitored by a Pirani gauge (10^{-6} mbar–1 bar) and is precisely measured in the pressure range encountered during flight ($\sim 10^{-4}$ –1 mbar) by a temperature-stabilized mks baratron. The temperature of the test gas is varied by means of liquid- N_2 cooling in the range from room temperature down to 180 K.

B. Calibration Results

An example of typical CO_2 and water-vapor $2f$ signals at three different total pressures (same mixing ratio) are shown in Fig. 9. The three features in this figure exhibit the typical shape expected for a $2f$ signal, i.e., similar to that of the second derivative of the absorption lines. The two absorption lines on the left-hand side of Fig. 9 correspond to CO_2 and the line on the right-hand side to H_2O . As expected, all three ab-

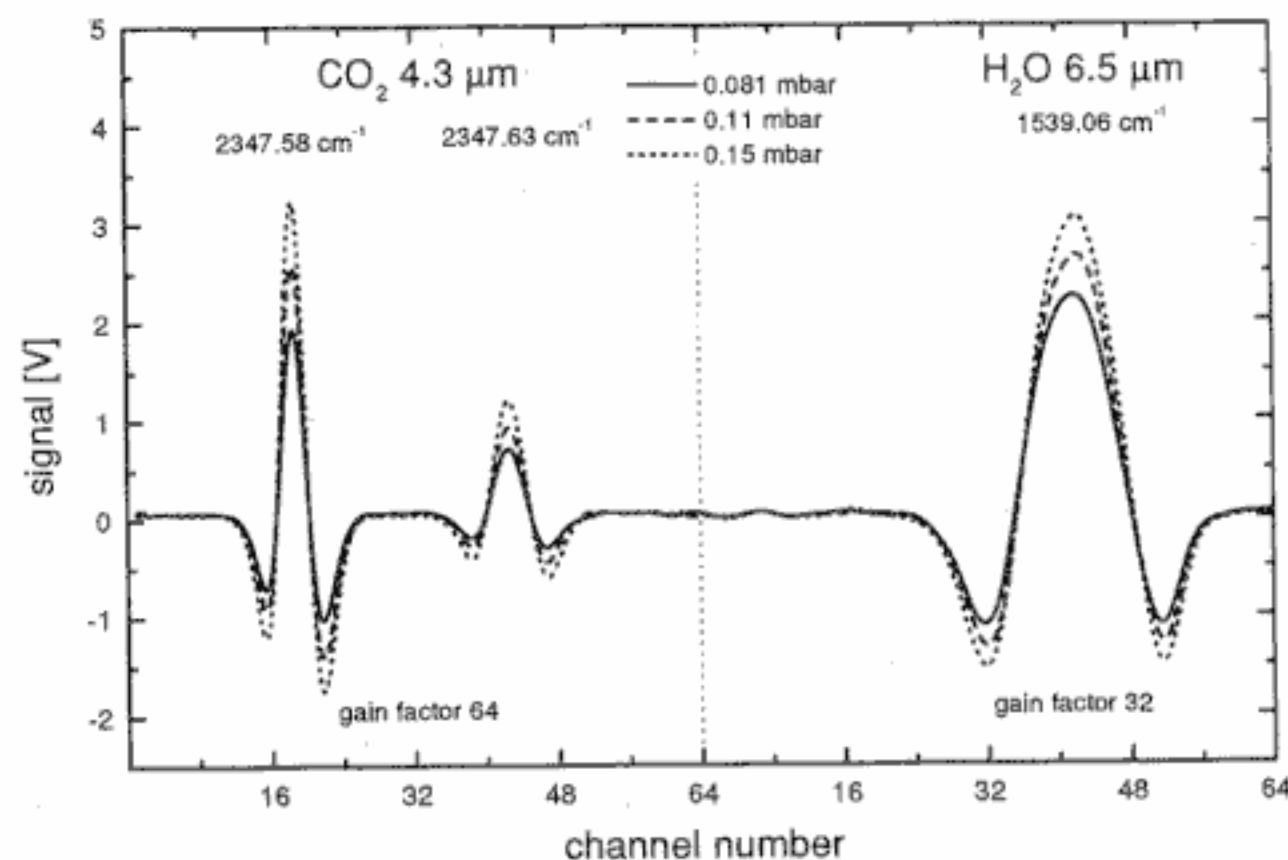


Fig. 9. $2f$ spectra of CO_2 and water vapor measured in the laboratory at three different total pressures (see inset) but constant mixing ratios. The two absorption lines at the left of the plot correspond to CO_2 , whereas the right line is caused by H_2O .

sorption lines show an increase of the signal with increasing pressure (constant mixing ratio).

In Fig. 10 the $2f$ signal amplitudes for the two CO_2 lines are shown as functions of the amount of gas (more precisely as functions of relative absorbance). Each point in this figure was obtained after 480 individual scans were averaged. As can be seen, the $2f$ signal amplitudes increase linearly with relative absorbance over 4 orders of magnitude, which demonstrates the large range of pressures within which the instrument can be used. The standard variation of the 480 individual signals from the mean is taken as a measure of instrumental noise and is used to determine the instrumental detection limit. We have performed statistical analyses of the absorption spectra that demonstrate that the noise is random. In particular the noise reduces proportionally to the square root of the integration time, at least for moderate integration times of up to a few seconds. For example, at time resolutions of 15 and 1000 ms we arrive at detection limits of $\sim 7 \times 10^{-4}$ and $\sim 8 \times 10^{-5}$, respectively $[(1000 \text{ ms}/15 \text{ ms})^{1/2} \sim 7 \times 10^{-4}/8 \times 10^{-5}]$. In summary, for an integration period of

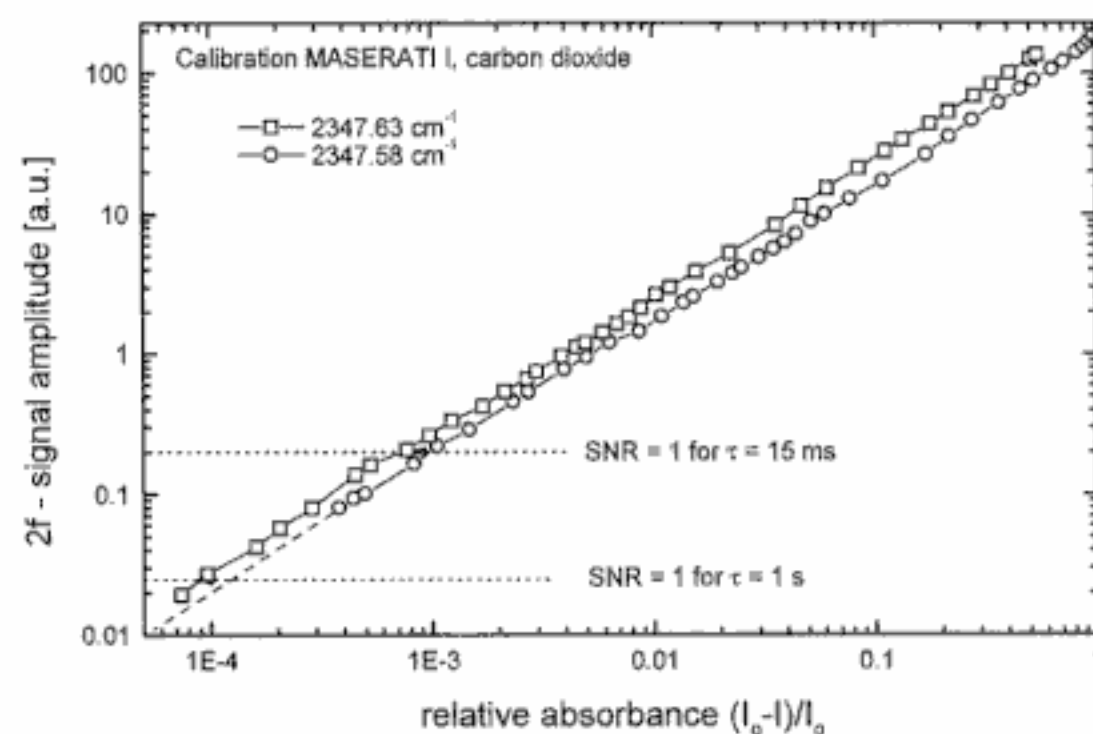


Fig. 10. Signal amplitude as a function of relative absorbance for the two CO_2 absorption lines shown in Fig. 9. The signal amplitudes increase linearly with the relative absorbances over 4 orders of magnitude. For a time resolution of 1 s, a detection limit below 1×10^{-4} is achieved.

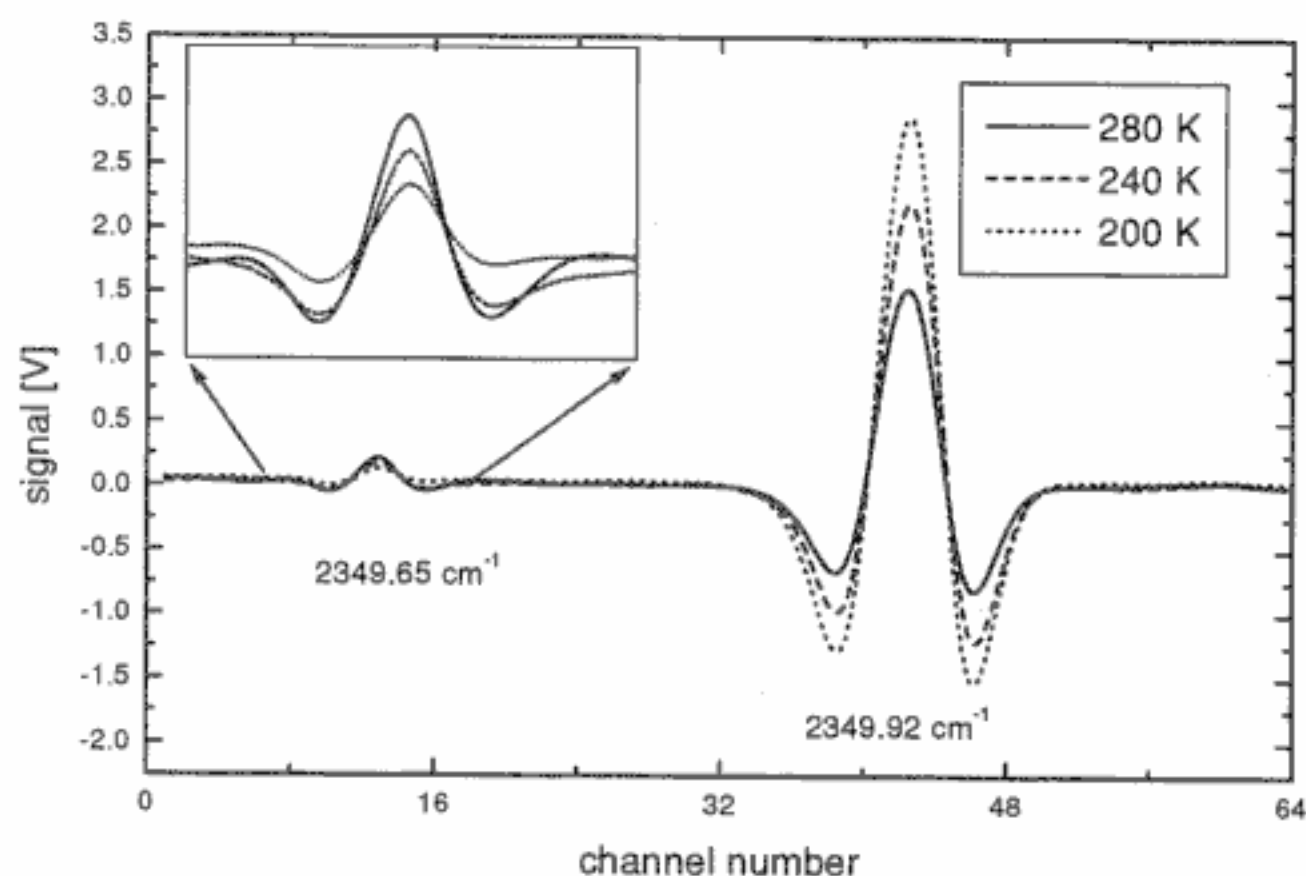


Fig. 11. Three scans of the two CO₂ lines recorded at different gas temperatures. Note that the left line increases with increasing temperature, whereas the right line decreases. This is due to the fact that the transition corresponding to the left absorption line starts from an excited level, whereas the right line starts from a ground level.

1 s (corresponding to an altitude resolution of 1 km during flight) the detection limit of our instrument is better than 10^{-4} . An even lower detection limit of 2×10^{-5} at a time resolution of 1 s is achieved in the water-vapor channel because of better laser performance.

We have performed flight simulation tests in our laboratory by varying the total pressure from less than 10^{-4} to 1 mbar in 1 min. The mixing ratio during each individual test was constant, but several runs for different mixing ratios of water vapor and CO₂ were carried out. These tests demonstrate the low response time of the instruments over a wide range of pressures. At conditions corresponding to altitudes below ~ 75 km the instrumental noise is smaller than approximately 1% of the signal (in the CO₂ channel), which is necessary to deduce atmospheric turbulence parameters from CO₂ number density fluctuations.

We have also studied the capabilities of the MASERATI instrument of measuring vibrational temperatures. For this purpose the gas temperature in the White cell was varied between 180 and 280 K to cover the range of temperatures expected in the atmosphere. In Fig. 11 the two CO₂ lines are shown at three different temperatures. Since the left line in the plot originates from an excited level (which is more populated when temperature increases) the absorbance at this line increases with increasing temperature (see inset in Fig. 11). For the other line (right-hand side of the plot) the situation is the other way around: It originates from a vibrational ground level that is depopulated when the temperature increases. The ratio of the two signal amplitudes is used as a measure of temperature, as is demonstrated in Fig. 12. The solid curve in this figure shows the theoretical curve that was normalized to the measurement at 240 K to eliminate a small difference in the amplifier gains. In general there is good agreement between the theoretical and the mea-

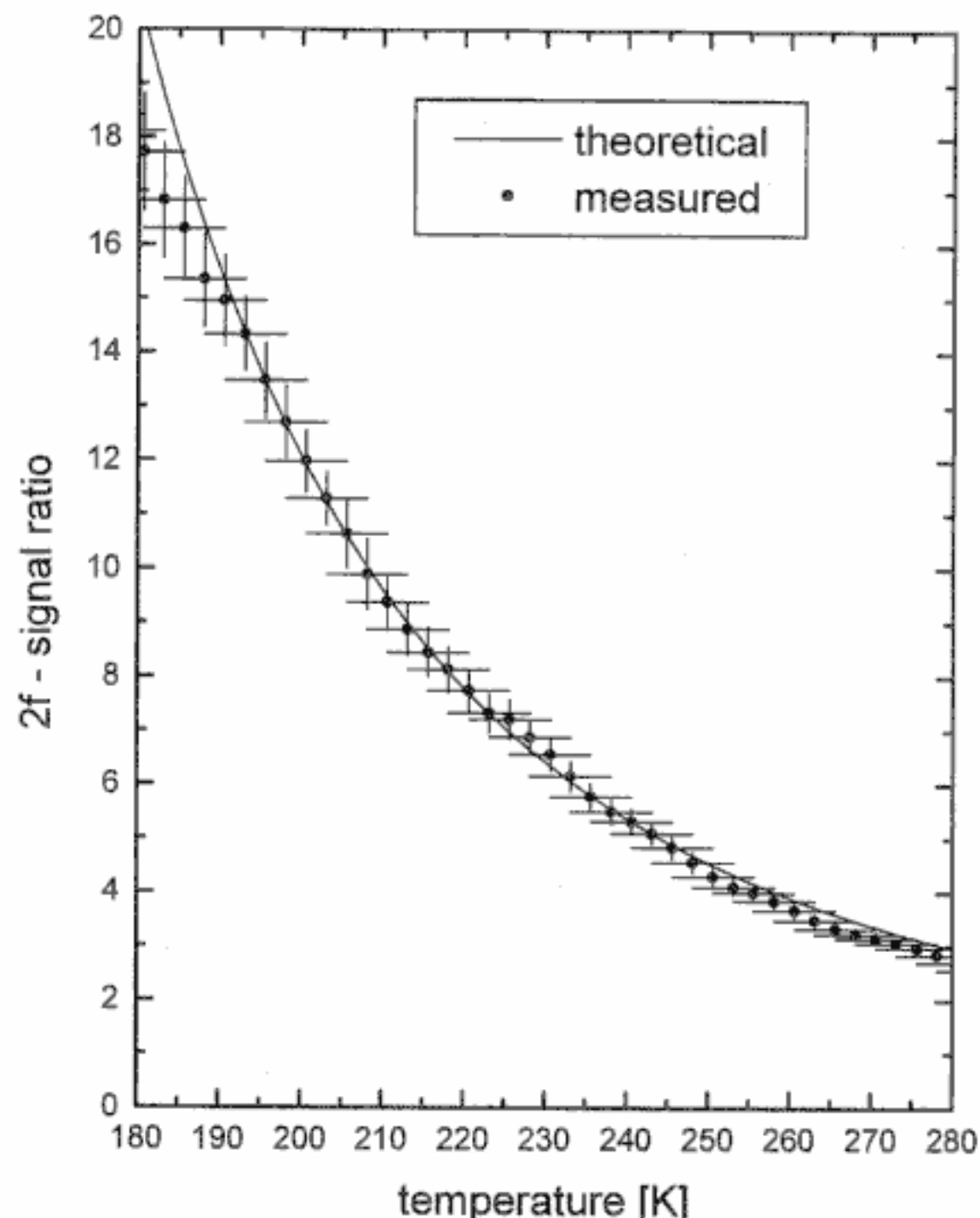


Fig. 12. Ratio of the signal amplitudes of the two CO₂ lines shown in Fig. 11 measured in the laboratory as a function of temperature (filled circles with error bars). The solid curve represents the theoretical curve normalized to the measurement at 240 K.

sured temperatures, which demonstrates that the MASERATI can be used to obtain temperatures at altitudes where the atmosphere is in LTE (the small deviation between the theoretical and the measured temperatures at very low temperatures in Fig. 12 is presumably due to the fact that the gas within the White cell is not equally thermalized).

6. Flight Performance

Two flights of the MASERATI instruments were performed on 12 October 1997, 01:19:00 UT, and on 31 January 1998, 23:43:00 UT, from the Andøya Rocket Range (69°N, 16°E). The launches took place under perfect operational conditions, i.e., no tropospheric clouds, little ground wind, no aurora. The rockets reached apogees of 120.9 and 118.9 km, respectively, which are close to the predicted value. Various falling spheres were launched before and after the RONALD flight to measure densities, temperatures, and horizontal winds in the mesosphere and the stratosphere. The Rayleigh-Mie-Raman lidar and the H₂O microwave spectrometer of the ALOMAR (Arctic Lidar Observatory for Middle Atmosphere Research) observatory were in operation during the RONALD launch period (see Ref. 19 for more details on the ALOMAR instrumentation).

In Table 3 the most important events happening during flight are listed; a nominal trajectory calculated for an elevation of 85° and a payload mass of 390 kg are assumed. Please note that the actual times and altitudes during the two flights are slightly different from those listed in the table. The rocket

Table 3. Events during the RONALD Flight^a

Flight Event	Time (s)	Altitude (km)
Ignition S-30 motor	0	0
Burnout S-30 motor	29	23.7
Despin 3 → 0.1 rps	47.5	47.5
TROLL door release	49.9	50
MASERATI cover separation	50	50.4
TROLL laser on	50.3	50.8
Separation S-30 motor	68.2	70
Apogee	172.3	121.4
Ignition recovery section	424.9	4.5
Impact motor	443	0

^aTimes and altitudes given correspond to a trajectory with nominal apogee (121.4 km) and departed slightly from these values during the two actual flights.

motor accelerates for ~29 s and reaches a maximum value of nearly 11 *g* shortly before burnout. At 47.5 s the spin of the rocket is reduced by a yoyo mechanism from 3 to 0.1 rps to avoid centrifugal forces on the multiple-pass absorption setup. The MASERATI starts atmospheric measurements on the upleg part of the flight at ~50 km after the cover is ejected. The payload falls into the open sea approximately 7.5 min after takeoff.

In Fig. 13 we show a sequence of 50 $2f$ signals from the H₂O channel measured early in the October 1997 flight. At this time the rocket is still accelerating with ~6 *g* and heavy vibrations occur in the entire payload. As can be seen from this figure, the $2f$ signal is very stable (rms deviation ~ 1%) despite the large mechanical stress on the MASERATI instrument (more details on this flight are given in Ref. 20). Unfortunately the separation of the nosecone failed so that the MASERATI instrument could not perform any atmospheric measurements.

In the second flight in January 1998 the nosecone (which includes the MASERATI cover) was successfully separated, and the MASERATI instrument performed perfectly, as is demonstrated in Fig. 14. Here, two CO₂ scans are shown, one shortly before

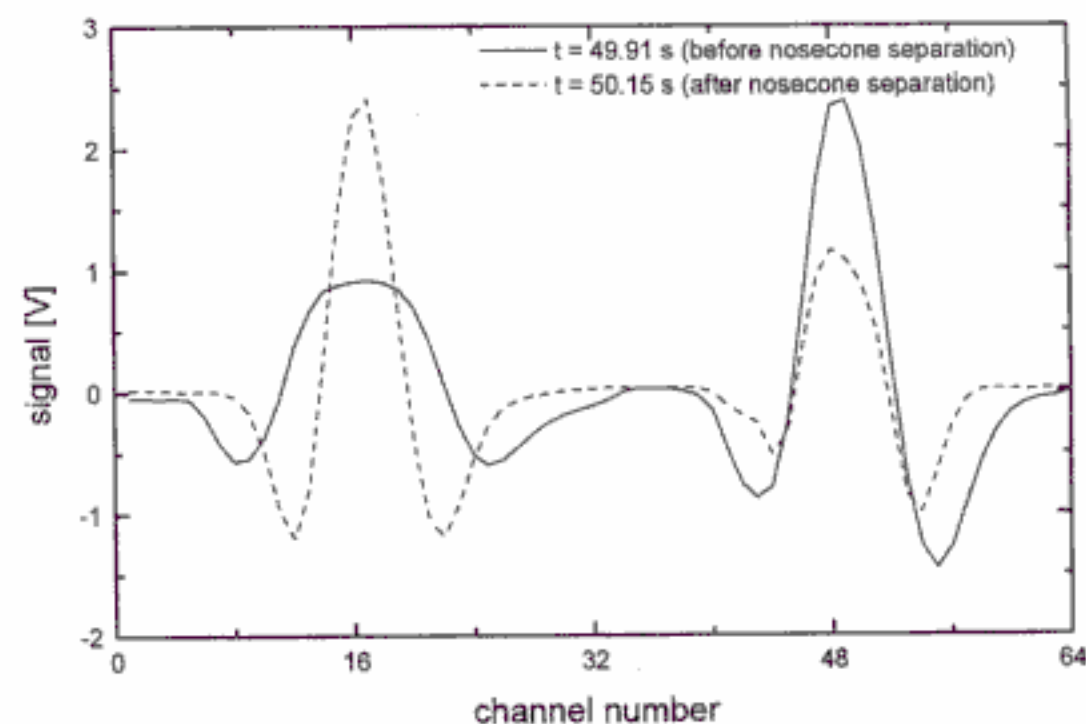


Fig. 14. Two CO₂ $2f$ spectra measured in the atmosphere during the second MASERATI flight on 31 January 1998. The spectra were measured immediately before and after nosecone separation, which occurred 50.0 s after lift-off. The shape of the spectra changes rapidly (within ≤15 ms) after nosecone release since the pressure in the vacuum cover (which is released together with the nosecone) is larger compared with the ambient pressure.

and the other shortly after the nosecone separation. The characteristics of the absorption lines immediately change when the cover is released since the pressure under the cover (~10 mbar) is larger compared with ambient (~1 mbar). Before the cover is released, the absorption lines are mainly pressure broadened, whereas after nosecone separation the linewidths shrink and are now determined by Doppler broadening.

The MASERATI instrument worked technically as expected when exposed to the atmosphere, as is demonstrated in Fig. 15. Here a sequence of 50 $2f$ scans of the CO₂ channel is shown as measured in the lower mesosphere at approximately 66–67 km. Again, very persistent and stable spectra (rms ~ 0.5%) are observed, which confirms the good technical performance of the MASERATI instrument. During this flight an unexpected signal increase of unknown origin was observed. A detailed analysis of the entire data set collected during this flight is currently under

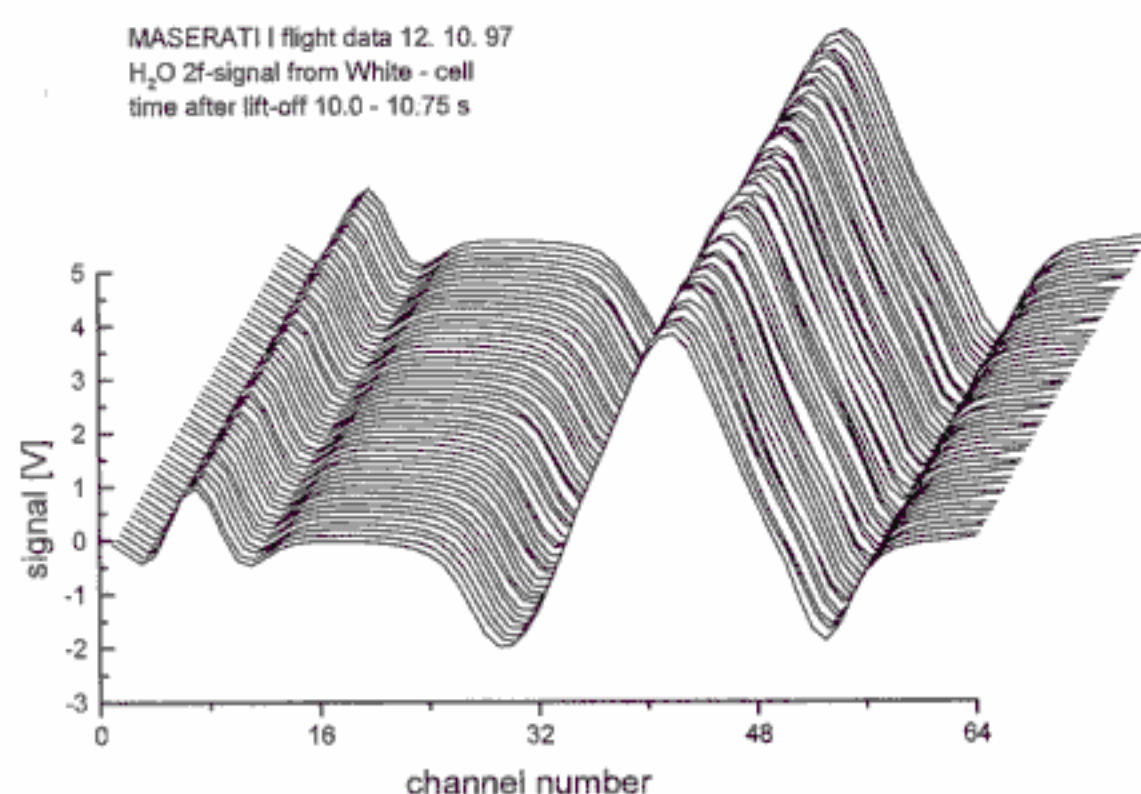


Fig. 13. Fifty successive $2f$ signals for H₂O measured in the White cell during the first MASERATI flight (time interval; 10–10.75 s after lift-off). Despite strong mechanical vibrations and large accelerations of approximately 6 *g*, the spectra are persistent and stable.

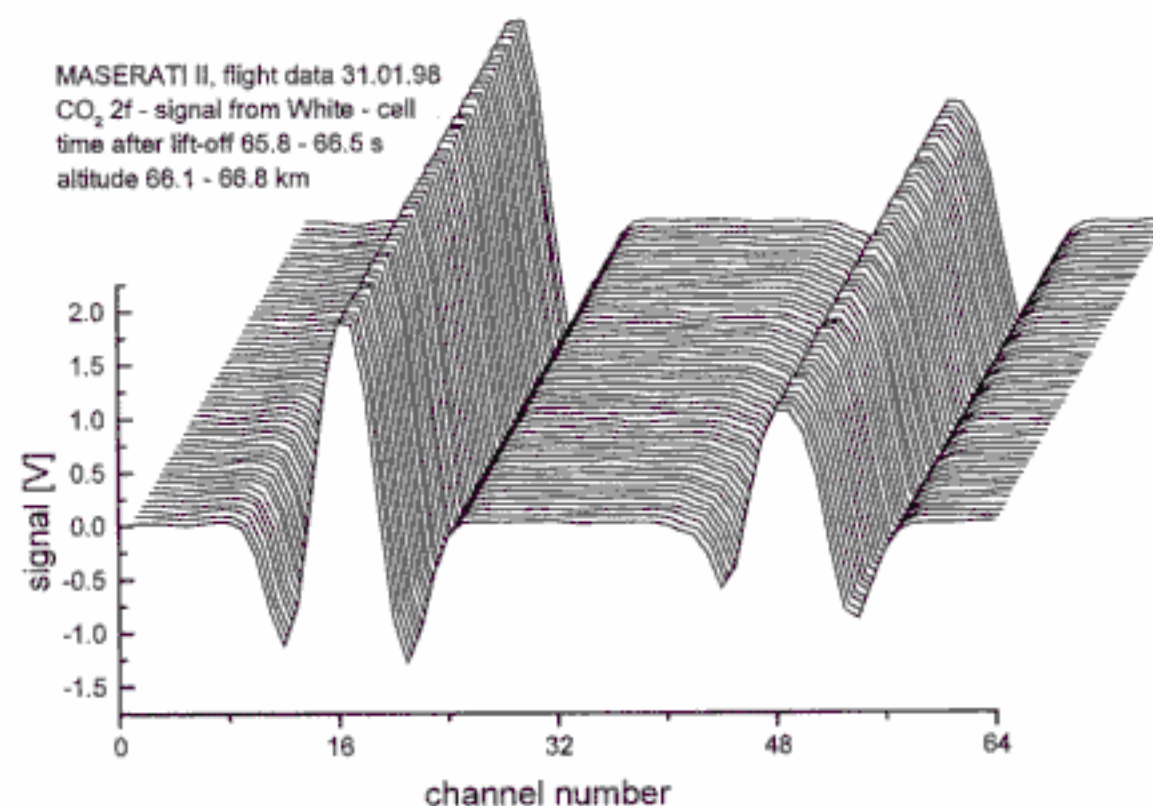


Fig. 15. Fifty successive $2f$ signals in the CO₂ channel measured in the atmosphere during the second MASERATI flight on 31 January 1998. These scans were recorded 65.8–66.5 s after lift-off, which corresponds to an altitude range of 66–67 km. Again, very persistent and stable spectra are measured with a maximum deviation of less than 1% from the mean.

way. Unfortunately, the sea recovery unit failed on both flights and the instruments could not be recovered.

7. Summary

A rocketborne tunable diode laser absorption spectrometer (TDLAS) system called MASERATI has been developed for measurements of H₂O and CO₂ in the MLT. The instrument has been specially designed, qualified, and tested to meet the strong requirements of an application on a sounding rocket. Two lead salt diode lasers are operated in a time-multiplex mode, and each gas is sampled approximately every 15 ms, which corresponds to an altitude resolution of ~15 m during the rocket flight. Frequency-modulation spectroscopy with lock-in detection is applied to achieve high sensitivity. An open multiple-pass absorption setup is mounted in front of the rocket, which ensures long optical path lengths with minimum physical space and guarantees instantaneous replacement of ambient air in the absorption path. Calibrations performed in our laboratory have shown that the absorption signal (more precisely, the $2f$ signal) is proportional to the gas abundance over a wide range of pressures. The smallest detectable relative absorbance is of the order of 10^{-4} – 10^{-5} (when spectra are integrated over 1 s), which is sufficient to measure H₂O up to ~90 km and CO₂ up to the apogee of the rocket flight (~120 km). We have demonstrated in the laboratory that the vibrational temperatures of the CO₂ molecules can be measured reliably by simultaneously scanning two CO₂ lines. This offers a new technique to obtain *in situ* temperature measurements in the upper mesosphere (where LTE prevails) and to study non-LTE effects in the lower thermosphere.

Two rocket flights with the new instruments were performed during winter 1997/1998 from northern Norway. The MASERATI instruments performed technically satisfactorily during these flights, which has demonstrated for, to our knowledge, the first time that the TDLAS technique is indeed suitable for *in situ* measurements in the MLT on board of sounding rockets. Some of the TDLAS features used in the MASERATI were specially designed for this project (e.g. the new Dewar and the open multiple-pass absorption setup) but are potentially useful also in other application, such as on aircrafts.

We thank R. Grisar, U. Klocke, M. Knothe, M. Tacke, and U. Ulmer as members of the TDLAS team at the Institut für Physikalische Messtechnik, Freiburg, Germany, for their continuous efforts during the development of the instruments, and von Hoerner & Sulger Electronics, Schwetzingen, Germany, for designing and producing major parts of the electronics. We are grateful to M. Rapp and R. Weingarten for their assistance during the laboratory tests and the shock-front calculations. We appreciate the support from the Mobile Raketenbasis of the Deutsches Zentrum für Luft- und Raumfahrt in Oberpfaffenhofen who built major parts of the

rocket hardware of the MASERATI. The personnel of the Andøya Rocket Range provided excellent support for the rocket launches. This development was supported by the Deutsche Agentur für Raumfahrt-Angelegenheiten, Bonn, under grant 50OE93016.

References

1. J. Y. N. Cho and J. Röttger, "An updated review of polar mesosphere summer echoes: observation, theory, and their relationship to noctilucent clouds and subvisible aerosols," *J. Geophys. Res.* **102**, 2001–2020 (1997).
2. M. Gadsden and W. Schroeder, *Noctilucent Clouds* (Springer-Verlag, Berlin, 1989).
3. K. U. Grossmann, "Mesospheric water vapor," in *Proceedings of the Sixth ESA Symposium on European Rocket and Balloon Programmes and Related Research*, ESA Spec. Pub. 183 (European Space Agency, Neuilly, France, 1983), pp. 83–87.
4. F.-J. Lübken, "MASERATI—a new rocketborne tunable diode laser experiment to measure trace gases in the middle atmosphere," in *Proceedings of the Tenth ESA Symposium on European Rocket and Balloon Programmes and Related Research*, ESA Spec. Pub. 317, 99–104 (European Space Agency, Neuilly, France, 1991), pp. 99–104.
5. H. Trinks and K. H. Fricke, "Carbon dioxide concentrations in the lower thermosphere," *J. Geophys. Res.* **83**, 3883–3886 (1978).
6. V. I. Fomichev, W. E. Ward, and C. McLandress, "Implication of variations in the 15 μ m CO₂ band cooling in the mesosphere and lower thermosphere associated with current climatologies of the atomic mixing ratio," *J. Geophys. Res.* **101**, 4041–4055 (1996).
7. F.-J. Lübken, W. Hillert, G. Lehmacher, U. von Zahn, M. Bittner, D. Offermann, F. Schmidlin, A. Hauchecorne, M. Mourier, and P. Czechowsky, "Intercomparison of density and temperature profiles obtained by lidar, ionization gauges, falling spheres, datasondes, and radiosondes during the DYANA campaign," *J. Atmos. Terr. Phys.* **56**, 1969–1984 (1994).
8. U. von Zahn, F.-J. Lübken, and Ch. Pütz, "BUGATTI experiments: mass spectrometric studies of lower thermosphere eddy mixing and turbulence," *J. Geophys. Res.* **95**, 7443–7465 (1990).
9. F.-J. Lübken, "On the extraction of turbulent parameters from atmospheric density fluctuations," *J. Geophys. Res.* **97**, 20385–20395 (1992).
10. P. Werle, "Spectroscopic trace gas analysis using tunable diode lasers," *Spectrochim. Acta A* **52**, 805–822 (1996).
11. R. T. Menzies, C. R. Webster, and E. D. Hinkley, "Balloonborne diode laser absorption spectrometer for measurements of stratospheric trace species," *Appl. Opt.* **22**, 2655–2664 (1983).
12. F. G. Wienhold, H. Fischer, P. Hoor, V. Wagner, R. Königstedt, G. W. Harris, J. Anders, R. Grisar, M. Knothe, W. J. Riedel, F.-J. Lübken, and T. Schilling, "TRISTAR—a tracer in-situ TDLAS for atmospheric research," *Appl. Phys. B* **67**, 411–417 (1998).
13. J. Reid, J. Shewchun, B. K. Garside, and E. A. Ballik, "High sensitivity pollution detection employing tunable diode lasers," *Appl. Opt.* **17**, 300–307 (1978).
14. T. Eriksen, U.-P. Hoppe, E. V. Thrane, and T. A. Blix, "Rocketborne Rayleigh lidar for *in situ* measurements of neutral atmospheric density," *Appl. Opt.* **38**, 2605–2613 (1999).
15. J. U. White, "Long optical paths of large aperture," *J. Opt. Soc. Am.* **32**, 285–288 (1942).

16. W. J. Riedel and M. Knothe, "Optics for tunable diode laser spectrometers," in *Measurement of Atmospheric Gases*, H. I. Schiff, ed., Proc. SPIE **1433**, 179–189 (1991).
17. D. Horn and G. C. Pimentel, "2.5-km low-temperature multiple-reflection cell," *Appl. Opt.* **10**, 1892–1898 (1971).
18. W. J. Riedel, M. Knothe, W. Kohn, and R. Grisar, "An anastigmatic White cell for IR diode laser spectroscopy," in *Proceedings of the International Symposium on Monitoring of Gaseous Pollutants by Tunable Diode Lasers* (Kluwer Academic, Dordrecht, The Netherlands, 1988), pp. 165–171.
19. U. v. Zahn, "Achievements of ALOMAR," in *Proceedings of the Thirteenth ESA Symposium on European Rockets and Balloon Programmes and Related Research*, ESA Spec. Pub. 397 (European Space Agency, Neuilly, France, 1997), pp. 141–163.
20. F.-J. Lübken, F. Dingler, and H. v. Lucke, "MASERATI: Experimental Method and First Results from a new Rocket-borne TDL Absorption Spectrometer" in *Proceedings of the 5th International Symposium on Gas Analysis by Tunable Diode Lasers*, Freiburg, 25–26. February 1998, organized by Fraunhofer Institut für Physikalische Meßtechnik IPM, Freiburg, Germany, and Verein Deutscher Ingenieure/Verein Deutscher Elektroingenieure - Gesellschaft Messund Automatisierungstechnik (VDI/VDE-GMA), VDI report, 1366, 101–110, Düsseldorf, Germany, 1998.